DISCRETE INVERSE METHOD FOR EXTRACTING DISEASE TRANSMISSION RATES FROM ACCESSIBLE INFECTION DATA*

XIUNAN WANG† AND HAO WANG‡

Abstract. Accurate estimation of the transmissibility of an infectious disease is critical to understanding disease transmission dynamics and designing effective control strategies. However, it has always been difficult to estimate the transmission rates due to the unobservability and multiple contributing factors. In this paper, we develop a data-driven inverse method based on discretizations of compartmental differential equation models for estimating time-varying transmission rates of infectious diseases. By developing iteration algorithms for three typical classes of infectious diseases, namely a disease with seasonal cycles, a disease with non-seasonal cycles, and a disease with no obvious periodicity, we demonstrate that the discrete inverse method is a valuable tool for extracting information from available pandemic or epidemic incidence data. We also obtain insights for some epidemiological phenomena and issues in concern based on each application. Our method is highly intuitive and generates rapid implementation even with multiple years of data instances. In particular, it can be used in conjunction with other data-driven technologies, such as machine learning, to forecast future disease dynamics based on future policies or human mobility trends, providing guidance to public health authorities.

Key words. inverse method, discretization, iteration, infectious disease, transmission rate, data-driven

AMS subject classifications. 92-08, 92B99

1. Introduction.

From the emergence of HIV in the 1980s to the recent COVID-19 pandemic, we have confronted a surge of catastrophic infectious diseases. Climate change, urbanization, global connectivity and fragile public health systems all accelerate the emergence of novel pathogens and cause the diseases to spread faster and wider than ever before [8, 10]. In order to mitigate the adverse impacts of infectious diseases on public health and economic growth, effective intervention strategies are urgently needed when an epidemic or pandemic strikes. This usually necessitates a precise estimate of the transmission rates of the diseases.

The transmission rate is a key important parameter in all compartmental infectious disease models which measures the transmissibility of the disease among a population. Transmissibility can not be observed or recorded directly and it can be influenced by many factors that are not easy to be included in a mathematical model, which makes the estimation of transmission rates extremely challenging. Our intuition about how contagious or deadly an infectious disease is comes from time series data of confirmed cases or mortality. However, such epidemiological data do not necessarily correlate to the severity of transmissibility and may mislead policymakers. When the notified number of new infections is small the disease may have already transmitted widely with a high transmission rate, with most people still in the incubation period or

*Submitted to Jon Rubin and Simone Bianco on May 25, 2022.

Funding: Research of XW is partially supported by Research and Creative Activity (RCA) Grant awarded by College of Arts and Sciences at the University of Tennessee at Chattanooga. Research of HW is partially supported by the Natural Sciences and Engineering Research Council of Canada (Individual Discovery Grant RGPIN-2020-03911 and Discovery Accelerator Supplement Award RGPAS-2020-00090) and the Canada Research Chair program (Tier 1 Canada Research Chair Award)

†Department of Mathematics, University of Tennessee at Chattanooga, Chattanooga, TN 37403, USA (xiunan-wang@utc.edu).

‡Corresponding Author. Department of Mathematical and Statistical Sciences, University of Alberta, Edmonton, AB T6G2G1, Canada (hao8@ualberta.ca).

asymptomatic and hence not being reported. In order to avoid a large-scale outbreak, immediate action is required in this situation. When the number of confirmed cases is large the transmission rate may be small if most people take more careful protection measures due to their awareness. Therefore, it is imperative to develop mathematical methodologies for extracting transmission rates from existing disease incidence data, with insights gained regarding disease transmission dynamics and the efficiency of public health interventions. Fortunately, the increasing availability of data resources makes the creation and application of such mathematical strategies possible.

Recently, several researchers have developed methods to estimate the temporally varying transmission rates based on differential equation models. Pollicott, Wang and Weiss [27] first introduced an inverse method for computing the continuous-time transmission rate by solving $\beta(t)$ from a Bernoulli differential equation derived from the model system. Hadeler [18] and Mubayi et al. [24] extended the method in [27] so that it applies to both prevalence and incidence data. Kong, Jin and Wang [19] built the inverse method algorithms for a new childhood measles model with applications to both pre-vaccination and post-vaccination data. All these works obtain a formula for $\beta(t)$ involving integrals which may require further discretization techniques and could become computationally extensive when applied to complex models. Compared to the continuous models, discrete models may provide a more reasonable and accurate approximation of the disease transmission dynamics since almost all data of infections are reported at discrete time points and the change of each compartment size, either as a population or as a frequency, is never continuous. In contrast to the "continuous" inverse methods, in this paper, we propose a highly tractable and fast "discrete" inverse method for estimating transmission rates of infectious diseases described by multi-compartmental difference equation models including quite complicated ones in which the transmission rate is not explicitly involved in the term corresponding to notification of new infections. We illustrate the idea by applying the approach to a general SIS model and show the applications of the method to three different diseases with distinct time series patterns: annual cycle, biennial cycle, and no apparent periodicity. For the continuous method, we also propose a more convenient way to realize the computation faster than those in [19, 27] when the term of notified new infections explicitly incorporates the transmission rate. Hopefully, this paper can provide hands-on guidance on estimating the transmission rates of various infectious diseases.

The rest of the paper is organized as follows. In Section 2, we show the derivations of the discrete inverse method based on forward, backward and centered Euler discretizations as well as the continuous inverse method and compare them in both accuracy and speed of computation for a general SIS model. In Section 3, we explain how the discrete inverse method works for a flu model based on incidence and vaccination data in the US from 2013 to 2018. In Section 4, we derive the algorithm of discrete inverse method for a general age-structured measles model incorporating birth and death and apply it to the measles data in London and Manchester, UK from 1950 to 1960. In Section 5, we use the discrete inverse method to estimate the transmission rate of SARS-CoV-2 Delta variant strain in California, USA from August to November 2021. At last, we discuss the advantages, limitations, and wide applicability of our method in Section 6.

2. Estimating the transmission rates from a general SIS model.

In this section, we derive the continuous inverse method and introduce the new discrete

inverse method based on the following general SIS model.

$$\begin{aligned} \frac{\mathrm{d}S(t)}{\mathrm{d}t} &= -\frac{\beta(t)S(t)I(t)}{N} + \gamma I(t), \\ \frac{\mathrm{d}I(t)}{\mathrm{d}t} &= \frac{\beta(t)S(t)I(t)}{N} - \gamma I(t), \end{aligned} \tag{2.1}$$

where S and I represent the susceptible and infected compartments, respectively. The total population size is N. γ is the recovery rate. $\beta(t)$ is the time-varying transmission rate.

2.1. Continuous inverse method. Motivated by [19, Theorem 4], we have the following theorem:

THEOREM 2.1. *For the SIS model (2.1), given a continuous function $\omega(t)$ generated from the incidence data, $\beta(t)$ can be estimated by $\frac{N\omega(t)}{S(t)I(t)}$ with $I(t)$ and $S(t)$ given by (2.4) and (2.5), respectively.*

Proof. Since $\frac{\beta(t)S(t)I(t)}{N} = \omega(t)$, system (2.1) is equivalent to

$$\begin{aligned} \frac{\mathrm{d}S(t)}{\mathrm{d}t} &= -\omega(t) + \gamma I(t), \\ \frac{\mathrm{d}I(t)}{\mathrm{d}t} &= \omega(t) - \gamma I(t). \end{aligned} \tag{2.2}$$

Solving the first equation of system (2.2), we get

$$S(t) = S(0) + \int_0^t (-\omega(s) + \gamma I(s))ds. \tag{2.3}$$

Solving the second equation of system (2.2) using the method of variation of parameters, we obtain

$$I(t) = I(0)e^{-\gamma t} + \int_0^t \omega(s)e^{\gamma(s-t)}ds. \tag{2.4}$$

Substituting (2.4) into equation (2.3), we obtain

$$S(t) = S(0) + \int_0^t \left(-\omega(s) + \gamma\left(I(0)e^{-\gamma s} + \int_0^s \omega(\tau)e^{\gamma(\tau-s)}d\tau\right)\right)ds. \tag{2.5}$$

∎

For the derivation of the continuous inverse method based on prevalence data, see supplementary Theorem SM0.1.

REMARK 2.2. *Indeed, when the term of notified new infections explicitly involves $\beta(t)$, it is not necessary to derive the analytic form of the solutions such as those obtained in the proof of Theorem 2.1 or in [19] in order to use the continuous inverse method to estimate the transmission rate. Instead, we can numerically solve the model system using ode45 in MATLAB once we obtain the splined curve of disease incidence data. After we get the time series values of the variables we can substitute them into the formula for the transmission rate. This will dramatically improve the speed of computation. However, if the term of notified new infections does not involve $\beta(t)$, we still need to derive the analytic form of the solutions first in order to apply the continuous inverse method, which could be rather complicated (see, e.g., supplementary Remarks SM0.3 and SM0.4). In both cases, our discrete inverse method is more powerful.*

2.2. Discrete inverse method. A discrete SIS model based on forward Euler discretization can be written

$$\begin{aligned} S_{n+1} &= S_n - \frac{\beta_n S_n I_n \Delta t}{N} + \gamma I_n \Delta t, \\ I_{n+1} &= I_n + \frac{\beta_n S_n I_n \Delta t}{N} - \gamma I_n \Delta t. \end{aligned} \tag{2.6}$$

By using the similar method as in the proof of [6, Lemma 2] and mathematical induction, we have the following lemma:

LEMMA 2.3. *Suppose that $S_0 > 0$, $I_0 > 0$ and $S_0 + I_0 = N$, then $S_n > 0$, $I_n > 0$ and $S_n + I_n = N$ if and only if $\gamma \Delta t \leq 1$ and $\beta_n \Delta t < (1 + \sqrt{\gamma \Delta t})^2$.*

THEOREM 2.4. *For the model system (2.6), suppose that the initial disease prevalence data I_0 is available and that the time series of incidence data y_n, $n = 0, 1, ..., K$, are given at equally spaced time step Δt, which satisfies $\gamma \Delta t \leq 1$ and $\beta_n \Delta t < (1 + \sqrt{\gamma \Delta t})^2$, then the transmission rates can be estimated by the following iteration process:*

$$\begin{aligned} I_{n+1} &= y_n \Delta t + (1 - \gamma \Delta t) I_n, \\ S_{n+1} &= N - I_{n+1}, \\ \beta_n &= \frac{N(S_n - S_{n+1})}{S_n I_n \Delta t} + \frac{N\gamma}{S_n}, \\ n &= 0, 1, ..., K - 1, \end{aligned} \tag{2.7}$$

and β_K can be approximated by β_{K-1}. Alternatively, the transmission rates can be estimated by

$$\beta_n = \frac{N y_n}{S_n I_n \Delta t}, \quad n = 0, 1, ..., K, \tag{2.8}$$

after the time series of S and I are derived.

Proof. Since $\frac{\beta_n S_n I_n}{N} = y_n$, $n = 0, 1, ..., K$, from the second equation of system (2.6) we have $I_{n+1} = y_n \Delta t + (1 - \gamma \Delta t) I_n$, $n = 0, 1, ..., K - 1$. Since $\gamma \Delta t \leq 1$ and $\beta_n \Delta t < (1 + \sqrt{\gamma \Delta t})^2$, by Lemma 2.3 we have $S_{n+1} = N - I_{n+1}$, $n = 0, 1, ..., K - 1$. Substituting S_{n+1}, S_n and I_n into the first equation of system (2.6), we can solve for β_n:

$$\beta_n = \frac{N(S_n - S_{n+1})}{S_n I_n \Delta t} + \frac{N\gamma}{S_n}, \quad n = 0, 1, ..., K - 1.$$

REMARK 2.5. *Theorem 2.4 provides two different ways for estimating the time series of transmission rates. The derivation in (2.7) does not depend on whether the term of notified new infections explicitly involves β_n, and hence, it is especially useful when the term representing notified incidence data is not described as $\beta(t)S(t)I(t)$ or $\frac{\beta(t)S(t)I(t)}{N}$, etc. (see, e.g., Sections 4 and 5). The advantage of using formula (2.8) is that β_K (i.e., the transmission rate at the end of the time interval) can also be derived from incidence data. However, (2.8) is only applicable when the term of notified new infections explicitly involves β_n.*

Next, we summarize the inverse method based on backward Euler discretization in parallel to (2.7). For the method based on centered Euler discretization, see

supplementary Theorem SM0.2. A discrete SIS model based on backward Euler discretization is given by

$$
\begin{aligned}
S_{n+1} &= S_n - \frac{\beta_{n+1} S_{n+1} I_{n+1} \Delta t}{N} + \gamma I_{n+1} \Delta t, \\
I_{n+1} &= I_n + \frac{\beta_{n+1} S_{n+1} I_{n+1} \Delta t}{N} - \gamma I_{n+1} \Delta t.
\end{aligned} \tag{2.9}
$$

THEOREM 2.6. *For the model system (2.9), suppose that the initial disease prevalence data I_0 is available and that the time series of incidence data y_n, $n = 0, 1, ..., K$, are given at equally spaced time step Δt, then the transmission rates can be estimated by the following iteration process:*

$$
\begin{aligned}
I_{n+1} &= \frac{y_{n+1}\Delta t + I_n}{1 + \gamma \Delta t}, \\
S_{n+1} &= N - I_{n+1}, \\
\beta_{n+1} &= \frac{N(S_n - S_{n+1})}{S_{n+1} I_{n+1} \Delta t} + \frac{N\gamma}{S_{n+1}}, \\
n &= 0, 1, ..., K-1,
\end{aligned}
$$

and β_0 can be approximated by β_1, if the obtained time series of susceptible and infected compartments as well as transmission rates are all non-negative, which can be tested numerically.

The proofs of Theorem 2.6 and supplementary Theorem SM0.2 can easily follow from that of Theorem 2.4.

2.3. Comparison of different discrete inverse methods and the continuous inverse method. Since the total population size does not change for the SIS system (2.1), we have $S(t) = N - I(t)$. An Itô stochastic differential equation model for the SIS epidemic process is

$$
\mathrm{d}I(t) = \left(\frac{\beta(t)(N - I(t))I(t)}{N} - \gamma I(t) \right) dt + \sqrt{\frac{\beta(t)(N - I(t))I(t)}{N} + \gamma I(t)} dW(t), \tag{2.10}
$$

where $W(t)$ is a Wiener process which depends continuously on t, $t \in [0, \infty)$.

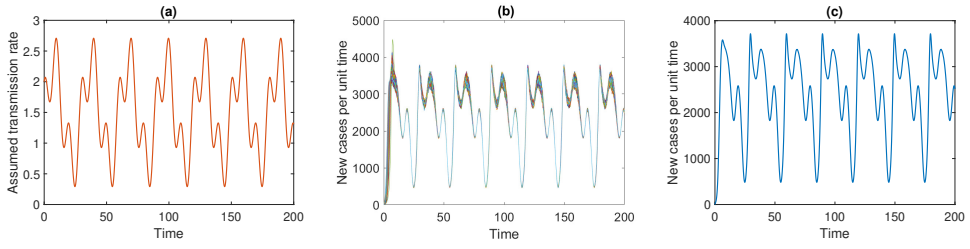

FIG. 2.1. *(a) A known time-varying transmission rate $\beta(t) = 1.5 + 0.5\cos\frac{\pi t}{5} + 0.8\sin\frac{\pi t}{15}$; (b) 1000 sample paths of model (2.10); (c) The average of the 1000 sample paths.*

Suppose that the time-varying transmission rate in (2.10) is given by $\beta(t) = 1.5 + 0.5\cos\frac{\pi t}{5} + 0.8\sin\frac{\pi t}{15}$ (see Figure 2.1 (a)). Then we can generate 1000 sample

paths of new infections per unit time (see Figure 2.1 (b)). Using the average of the 1000 sample paths of new infections per unit time in Figure 2.1 (c) as the incidence data, we estimate the transmission rate by using the discrete inverse method based on forward, backward and centered Euler discretizations as well as the continuous inverse method. We set $N = 8000$, $\gamma = 0.5$ and take the time step as $\Delta t = 0.05$. The continuous inverse method and discrete inverse method based on forward Euler and backward Euler discretizations produce almost the same transmission rates for the general SIS model as shown in Figure 2.2. However, negative values occur for the transmission rates estimated by the discrete inverse method based on centered Euler discretization (see supplementary Figure SM0.1). Thus, the centered Euler discretization does not work well for model (2.1) with the given time step.

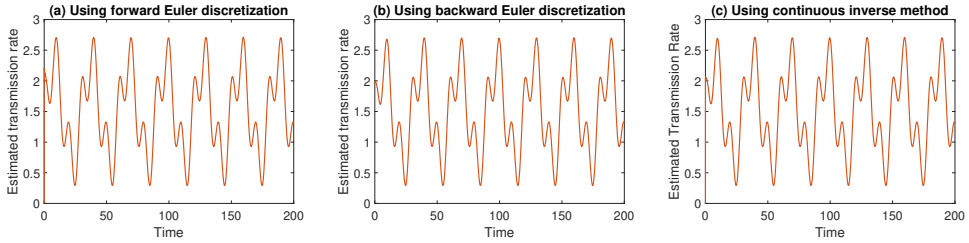

FIG. 2.2. *The estimated transmission rates: (a) by discrete inverse method based on forward Euler discretization; (b) by discrete inverse method based on backward Euler discretization; (c) by continuous inverse method.*

To evaluate the accuracy of each method, we use the mean absolute error (MAE) to compute the differences between the assumed transmission rate and those obtained by the inverse methods. The formula of MAE is given by

$$\text{MAE} = \frac{1}{n}\sum_{i=1}^{n}|z_i - x_i|,$$

where x_i is the i-th component of the vector of assumed transmission rates, z_i is the i-th component of the vector of estimated transmission rates, and n is the total number of data instances. The comparison of different methods in accuracy and speed is shown in Table 2.1, from which we can see that all the three methods generate accurate results while the discrete inverse method based on forward Euler discretization is the fastest.

	Forward Euler	Backward Euler	Continuous method
MAE	0.0025	0.0074	0.0045
Time elapsed (seconds)	0.0055	0.0064	0.2272

TABLE 2.1
Comparison of the methods for SIS model in accuracy and speed.

3. Application to a disease with seasonal cycles. Seasonality is a ubiquitous feature of many infectious diseases such as influenza (flu), cholera, malaria, dengue fever, etc. In this section, we show how to use the discrete inverse method to estimate the transmission rate of flu in the US. Traditional flu models usually

adopt an S-I structure without considering the impact of vaccination (see, e.g., [31]). However, in the US, about half population gets flu vaccines each year and some vaccinated people can still get infected. Accordingly, we develop a flu model with five compartments: susceptible (denoted by S), infected (I), vaccinated but not infected (V), recovered (R) and dead (D). The transmission rate $\beta(t)$, the vaccination rate $\alpha(t)$ and the death rate $\mu(t)$ are all time-varying parameters. The total population N and the recovery rate γ are assumed to be constant. Since vaccines against influenza do not provide complete protection [15], both susceptible and vaccinated individuals will enter the infectious compartment after getting infected. The relative risk of infection for vaccinated individuals compared to susceptible ones is ϵ. For people who are unvaccinated, if they get infected with flu, then their recovery time and the chance of death may vary depending on their immunity. So we put vaccinated-infected and unvaccinated-infected individuals in one compartment–"I" although the symptoms of vaccinated individuals with infection are mild such that almost no death would occur and they also recover faster [15]. In other words, we assume that the differences in recovery and infection-induced mortality are negligible between vaccinated-infected and unvaccinated-infected individuals. The model is given as follows:

$$
\begin{aligned}
\frac{\mathrm{d}S(t)}{\mathrm{d}t} &= -\frac{\beta(t)S(t)I(t)}{N} - \alpha(t)S(t),\\
\frac{\mathrm{d}I(t)}{\mathrm{d}t} &= \frac{\beta(t)(S(t)+\epsilon V(t))I(t)}{N} - \gamma I(t) - \mu(t)I(t),\\
\frac{\mathrm{d}V(t)}{\mathrm{d}t} &= \alpha(t)S(t) - \frac{\epsilon\beta(t)V(t)I(t)}{N},\\
\frac{\mathrm{d}R(t)}{\mathrm{d}t} &= \gamma I(t),\\
\frac{\mathrm{d}D(t)}{\mathrm{d}t} &= \mu(t)I(t).
\end{aligned}
\tag{3.1}
$$

Since people with uncomplicated flu symptoms typically recover within 7 days although cough and malaise can last longer especially in those with lung disease and elderly people [15], we assume that the average length of the infectious period is 7 days, that is, $\gamma = 1$ per week. The CDC conducts research every year to evaluate how effective the flu vaccines are at protecting people from the virus. While vaccine effectiveness varies, recent research demonstrates that flu vaccination reduces the risk of flu sickness by 40% to 60% in the general population during seasons when the viruses used to manufacture flu vaccines matched well to the majority of circulating ones [15]. Appropriately, we set $\epsilon = 0.5$. Note that we do not need to estimate the vaccination rate $\alpha(t)$ and death rate $\mu(t)$ because we can directly use the vaccination and mortality data, both of which are available from CDC (see [15]). We collected weekly data about new infections, cumulative vaccinated and deaths in the US from week 35 of 2013 to week 34 of 2018. Since the circulating virus strains are usually different among different years [15], we assume that individuals in the "R" compartment are immune against the virus strains only in the present flu season year. In addition, considering that there is large variations of the total US population in consecutive years, we use different total population sizes to estimate the transmission rates for different flu seasons. For example, we assume that the population in the 2013-2014 flu season is approximately equal to the population in 2013 and that the population in the 2014-2015 flu season is approximated by the population in 2014, and so forth. By doing this, we can neglect the natural birth and death rate as well as immigration/emigration

rate in the model. Table 3.1 gives the values of N for different flu seasons:

	2013-2014	2014-2015	2015-2016	2016-2017	2017-2018
Population	316129000	319113000	321442000	323100000	325719000

TABLE 3.1
Total population of the United States for each flu season year.

In order to use the continuous inverse method to estimate the transmission rate, we need to derive an equivalent system which does not explicitly involve $\beta(t)$. Suppose that $y(t)$ is the reported number of new infections per unit time at time t which can be obtained by a spline of the time series of weekly new infections. It follows that

$$y(t) = \frac{\beta(t)(S(t) + \epsilon V(t))I(t)}{N}.$$

The proportion of new infections from the susceptible is $\frac{S(t)}{S(t)+\epsilon V(t)}$ and the infections from the vaccinated account for a proportion of $\frac{\epsilon V(t)}{S(t)+\epsilon V(t)}$. Then the model system (3.1) can be approximated by the following system:

$$\begin{aligned}
\frac{\mathrm{d}S(t)}{\mathrm{d}t} &= -\frac{S(t)y(t)}{S(t) + \epsilon V(t)} - u(t),\\
\frac{\mathrm{d}I(t)}{\mathrm{d}t} &= y(t) - \gamma I(t) - d(t),\\
\frac{\mathrm{d}V(t)}{\mathrm{d}t} &= u(t) - \frac{\epsilon V(t)y(t)}{S(t) + \epsilon V(t)},\\
\frac{\mathrm{d}R(t)}{\mathrm{d}t} &= \gamma I(t),\\
\frac{\mathrm{d}D(t)}{\mathrm{d}t} &= d(t),
\end{aligned} \tag{3.2}$$

where $u(t)$ and $d(t)$ are the splined functions of weekly new vaccinated and new deaths, respectively. After we numerically solve for $S(t)$, $I(t)$ and $V(t)$ from system (3.2), we can find the transmission rate:

$$\beta(t) = \frac{Ny(t)}{(S(t) + \epsilon V(t))I(t)}.$$

Next, we estimate the transmission rates by using the discrete inverse method based on forward Euler discretization of system (3.2). For each flu season year (starting from week 35 of the former year), let $y[i]$ be the number of newly infected individuals in the i-th week, $i = 1, 2, ..., K$, where $K = 53$ for the flu season year 2014-2015 and $K = 52$ for the other years. Then $y[i]$, $i = 1, 2, ..., K$, can be approximated by the number of patients consulting with influenza like illness (ILI) each week reported by CDC [15] (see supplementary Figure SM0.3). We use $S[i]$, $I[i]$, $V[i]$, $R[i]$, $D[i]$ to represent the values of variables in model (3.1) in the i-th week, and use $u[i]$ and $d[i]$ to represent the number of newly vaccinated and new deaths in the i-th week, $i = 1, 2, ..., K$. We can derive the time series of $u[i]$, $i = 1, 2, 3, ..., K$, according to the data of cumulative vaccinated population and obtain the time series data of $d[i]$, $i = 1, 2, ..., K$, from CDC [15]. For each flu season year, we take the initial values of the variables as follows:

(i) $R[1] \approx 0$ because we assume that recovered individuals in the last flu season year is no longer immune to the flu virus strain in the present year;
(ii) $I[1] \approx$ the number of new infections in the first week (i.e., in week 35 of the former year);
(iii) $D[1] \approx$ the number of new flu-related deaths in the first week (i.e., in week 35 of the former year);
(iv) $V[1] \approx$ the cumulative number of vaccines given in the corresponding flu season by the end of the first week (i.e., by week 35 of the former year).

It follows that

$$S[1] = N - I[1] - V[1] - R[1] - D[1] \quad \text{and} \quad \beta[1] = \frac{Ny[1]}{(S[1] + \epsilon V[1])I[1]}.$$

With these initial values, we can run the following iteration:

$$\begin{aligned}
I[i] &= I[i-1] + y[i-1] - \gamma I[i-1] - d[i-1], \\
V[i] &= V[i-1] + u[i-1] - \frac{\epsilon V[i-1] y[i-1]}{(S[i-1] + \epsilon V[i-1])}, \\
R[i] &= R[i-1] + \gamma I[i-1], \\
D[i] &= D[i-1] + d[i-1], \\
S[i] &= N - I[i] - R[i] - D[i] - V[i], \\
\beta[i] &= \frac{Ny[i]}{(S[i] + \epsilon V[i])I[i]},
\end{aligned}$$

for $i = 2, 3, ...K$.

Figure 3.1 (a) shows the estimated transmission rates for each flu season year. In Figure 3.1 (b) we classify the transmission rates using box plots where each box corresponds to one flu season. The transmission rates in 2013-2014 have the smallest median and variation compared to those in the subsequent years. Although the medians in 2016-2017 and 2017-2018 are a little smaller than that in 2015-2016, the peak transmission rate and the upper quartile are increasing. The boxes become comparatively longer and longer by years. This could be due to climate change in recent years, which makes the transmission rates vary dramatically due to some abnormal variations of temperatures and leads to an increasing number of people infected with flu in some states. We can see in supplementary Figure SM0.3 that the total number of weekly ILI cases keeps increasing since the flu season in 2015 and the peak in 2017-2018 is much higher than those peaks in former years. In Figure 3.2 (a) we put these transmission rates consecutively from week 35 of 2013 to week 34 of 2018. Figure 3.2 (b) gives the modulus of Fourier transform of the transmission rate series. We can see that the dominant frequency is 1/year, which is consistent with the common opinion that flu is a seasonal disease.

In Figure 3.3, we classify the transmission rates from 2013 to 2018 by month. The maximum, upper quartile and median of transmission rates in August are higher than those in September. In the fall, with more and more people get vaccinated combined with education campaigns such as attention of hygiene habits, the tranmssion rates drop in September. However, as the weather becomes colder, the environment becomes increasingly favorable for the transmission of influenza virus so that the transmission rates keep increasing in the fall as shown in Figure 3.3. The transmission rates are largest in December in terms of the maximum, upper quartile,

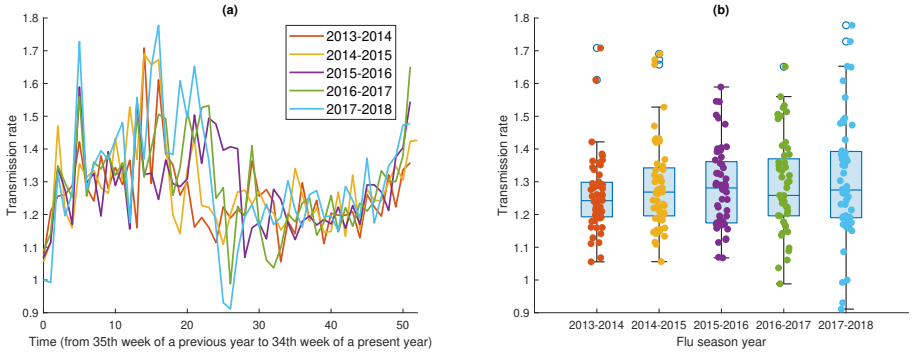

FIG. 3.1. *The transmission rates of flu in the US for each flu season year.*

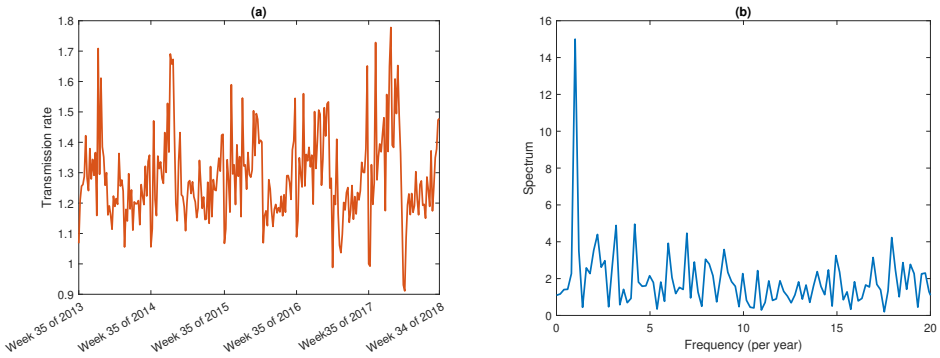

FIG. 3.2. *(a) The transmission rates of flu in the US from week 35 of 2013 to week 34 of 2018. (b) The modulus of Fourier transform of the transmission rates from week 35 of 2013 to week 34 of 2018.*

median, lower quartile and minimum. Thus, public health agencies should take effective measures and extra attention against flu in December each year in the US. Some non-pharmaceutical interventions, such as recommendation of facial masks, may be worth implementing in December. We can also observe that the transmission rates start to drop in January and February each year although the temperature is still low. This may be because the number of vaccinated population usually arrives at the peak around the end of December so that some communities are well protected.

A comparison of the transmission rates obtained by discrete and continuous inverse methods is shown in Figure 3.4 and the time elapsed for running each algorithm for each flu season year is given in Table 3.2. We can see that the curve obtained by the continuous method is smoother since it is derived by using the splined functions of known data. Although there are some differences in the values of the estimated transmission rates, the two methods give the same trends of the transmission rate which can provide the same guiding information for policymakers in designing disease control measures since what really matters in disease control is to know when the transmission rate will increase, when it will decrease, and when it will arrive at a peak value.

4. Application to a disease with non-seasonal cycles. Some infectious diseases, such as measles and pertussis, can display outbreaks in multi-year intervals

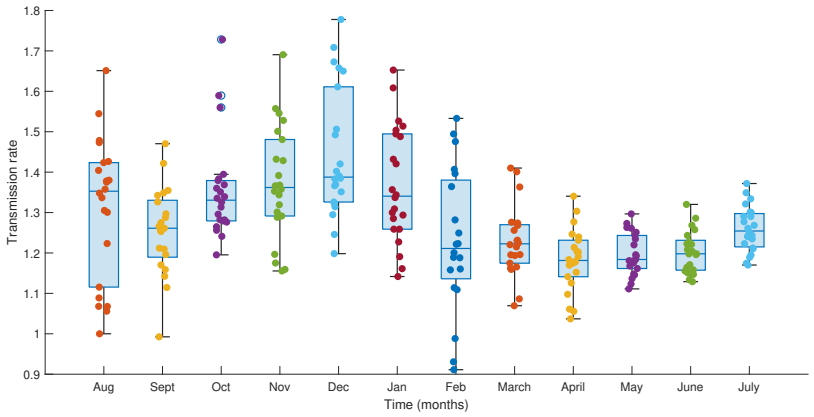

FIG. 3.3. *The boxplot of transmission rates of flu in the US for each month from 2013 to 2018.*

	2013-2014	2014-2015	2015-2016	2016-2017	2017-2018
Discrete	0.0178	0.0115	0.0123	0.0149	0.0119
Continuous	0.1010	0.1240	0.1270	0.1290	0.1149

TABLE 3.2

Comparison of the time elapsed (in second) for estimating the transmission rates of flu in the US by discrete and continuous inverse methods.

rather than annually because the timing of these epidemics is regulated by a combination of seasonal transmission and various processes determining the size of the susceptible compartment in a population, which must be sufficiently large for an outbreak to occur [23]. In this section, we derive the algorithm of the discrete inverse method for estimating the transmission rates of measles, a common childhood infectious disease with biennial cycles.

Most existing measles models assume a homogeneous mixing of infections among children and adults (see, e.g., [9]) although measles is an obvious childhood disease. Motivated by the model in [19], we develop an age-structured measles transmission model by assuming that only unvaccinated juvenile population are susceptible to measles. We partition the population into two groups: adult (denoted by A) and juvenile. The juvenile population consists of four compartments: susceptible (S), exposed (E), infectious (I), and recovered/ vaccinated (R). We use the variables to represent the frequency or proportion of individuals in each compartment among the entire population instead of the population size of each compartment. We consider both birth rate (λ) and natural death rate (δ) so that we can estimate the transmission rate for multiple years or even longer by using one set of initial values. Considering that children normally do not die naturally, we ignore the death rate of the juvenile population. Instead, we consider a growth rate (g) for the juvenile population. People above the age of $1/g$ are in the adult group and they are no longer susceptible to measles. In addtion, we denote the disease-induced death rate as μ. We assume that a proportion p of the new borns are vaccinated against measles. Let the transition rate from E to I be $aE(t)$ and that from I to R be $vI(t)$. Then $1/a$ is the length of the incubation period, and $1/v$ represents the length of the infectious period. We

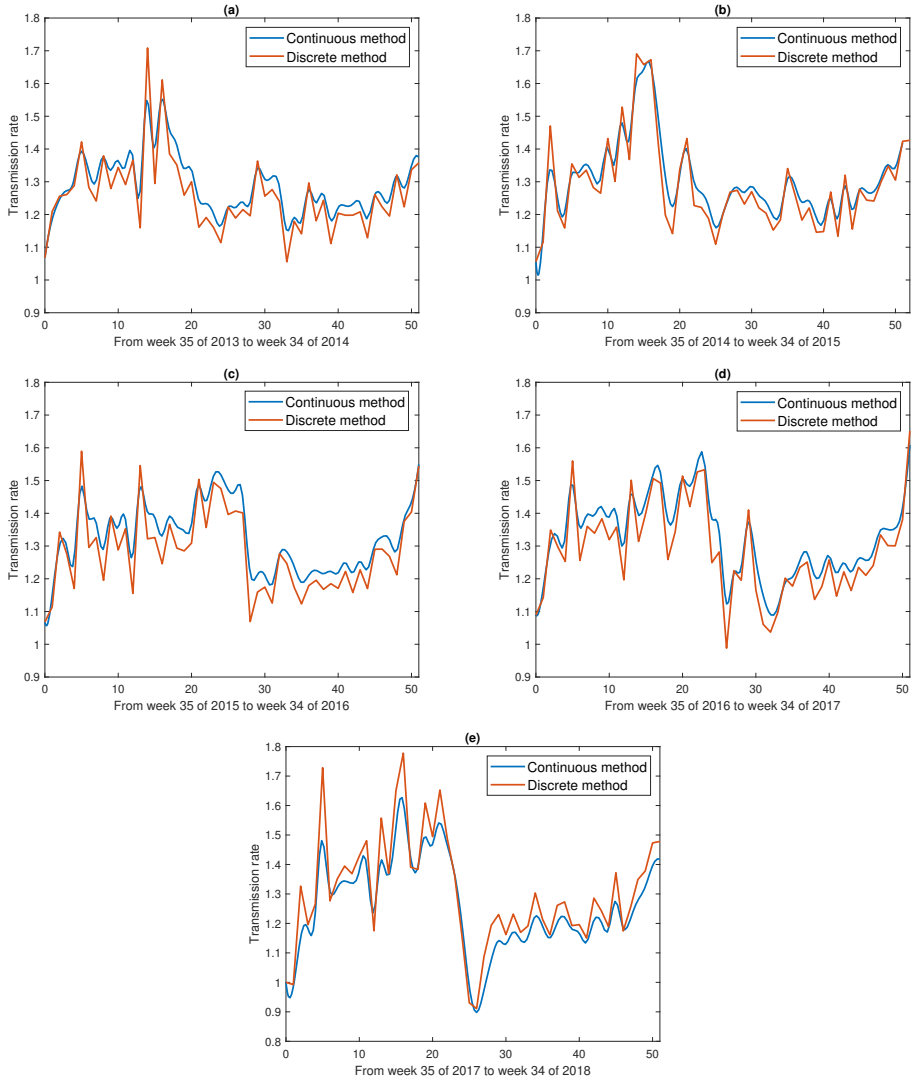

FIG. 3.4. *Comparison of the transmission rates of flu in the US estimated by discrete and continuous inverse methods for each flu season year.*

aim to estimate the time-varying transmission rate $\beta(t)$ by using the discrete inverse method. The model is given by the following system of differential equations:

$$
\begin{aligned}
\frac{\mathrm{d}S(t)}{\mathrm{d}t} &= (1-p)\lambda A(t) - \beta(t)S(t)I(t) - gS(t),\\
\frac{\mathrm{d}E(t)}{\mathrm{d}t} &= \beta(t)S(t)I(t) - aE(t) - gE(t),\\
\frac{\mathrm{d}I(t)}{\mathrm{d}t} &= aE(t) - vI(t) - gI(t) - \mu I(t),\\
\frac{\mathrm{d}R(t)}{\mathrm{d}t} &= p\lambda A(t) + vI(t) - gR(t),\\
\frac{\mathrm{d}A(t)}{\mathrm{d}t} &= g(S(t)+E(t)+I(t)+R(t)) - \delta A(t).
\end{aligned} \tag{4.1}
$$

Let $y[i]$ be the notification data of new infections, $S[i]$, $E[i]$, $I[i]$, and $R[i]$ represent the frequency of susceptible, exposed, infectious, and recovered/vaccinated juvenile individuals, respectively, and $A[i]$ the frequency of adult ones in the i-th week, $i = 1, 2, ..., K$, where K is the length of the notification data vector. Considering that measles are suspected in patients presenting with common symptoms such as rash and high fever which appear during the infectious period [14], we can assume that $aE[i] = y[i]/N[i]$. Then $E[i] = y[i]/aN[i]$, $i = 1, 2, ..., K$, where $N[i]$ represents the total population in the i-th week.

Suppose that we know the initial value of each variable, then we can obtain $I[i]$, $R[i]$, $A[i]$ and $S[i]$ by the following iteration process:

$$
\begin{aligned}
I[i] =& I[i-1] + aE[i-1] - (v+g+\mu)I[i-1],\\
R[i] =& R[i-1] + p\lambda A[i-1] + vI[i-1] - gR[i-1],\\
A[i] =& A[i-1] + g(S[i-1] + E[i-1] + I[i-1] + R[i-1]) - \delta A[i-1],\\
S[i] =& 1 - E[i] - I[i] - R[i] - A[i].
\end{aligned}
$$

for $i = 2, 3, ...K$.

Discretizing the first equation of system (4.1), we have

$$
\begin{aligned}
&S[i] - S[i-1]\\
=&(1-p)\lambda A[i-1] - \beta[i-1]S[i-1]I[i-1] - gS[i-1], \quad i = 2, 3, ..., K.
\end{aligned}
$$

It follows that

$$
\beta[i-1] = \frac{(1-g)S[i-1] - S[i] + (1-p)\lambda A[i-1]}{S[i-1]I[i-1]}, \quad i = 2, 3, ..., K,
$$

and $\beta[K] \approx \beta[K-1]$.

In what follows, we use the above algorithm to estimate the tranmission rate of measles in London and Manchester, UK from 1950 to 1960 based on the notification data of weekly new cases obtained from [13] (see supplementary Figure SM0.10) with a standard correction factor of 92.3% due to a mean reporting rate of 52% for UK measles cases [12]. Note that $92.3\% = 1/0.52 - 1$. The metro area populaions of London and Manchester in 1950 are approximately 8361000 and 2422000, respectively. Since the metro area populations of these two cities almost have no change in 1950s, with the annual changes as low as -0.21% to 0.00% for London (see [20]) and 0.00% to 0.04% for Manchester (see [21]), we assume that the birth rate and natural death rate are equal: $\lambda = \delta = 1/(68.69 \times 52)$ per week, where 68.69 is the average life

expectancy of UK in 1950s [22]. According to [37], the majority of disease-induced deaths of measles occur among young children with insufficient nourishment or weakened immunity due to HIV/AIDS and other diseases and usually happen in developing countries with low per capita incomes and poor health infrastructures. Since UK is a developed country, it is reasonable to assume that $\mu = 0$. Note that in 1950s vaccination has not been carried out in London, which gives $p = 0$. We take the value of a from [7, 26]: $a = 1$ per week. An infected individual is able to transmit measles starting four days before the rash occurs and ending four days after the rash errupts [37]. Thus, we can assume that the infecious period is approximately 8 days, that is, $v = 7/8$ per week. Since the infectious period of measles is about 8 days, we estimate $I[1]$ to be the sum of the number of reported new cases in the last week of 1949 and in the first week of 1950. We assume that $R[1] = 1000I[1]$. According to [28], the population above the age of 16 in UK in 1950 accounts for about 74.3%. Thus, we assume that $A[1] = 0.743$ and $S[1] = 0.257 - E[1] - I[1] - R[1]$ for both London and Manchester.

The estimated transmission rates of measles in London and in Manchester compared with the holiday seasons from 1950 to 1960 are presented in Figure 4.1. Most peak values of the transmission rates appear during school terms. In particular, it is easy to observe that the transmission rates decrease to a lower level during most summer holidays and bounce back to an upper level when the school terms resume.

Figure 4.2 shows the modulus of the Fourier transform of the transmission rates in London and in Manchester from 1950 to 1960. The modulus has two dominant frequencies: 1/year and 3/year, which is consistent with the findings of [19]. The 1/year peak is much higher than the 3/year peak in Figure 4.2 (a) which indicates that measles in London is mainly influenced by seasonal factors such as temperature, rainfall and humidity. The 3/year peak shows that school terms also play an indispensable role in the transmission of measles since schools in UK have three terms each year: Autumn term (from early September to mid December), Spring term (from early January to late March or early April) and Summer term (from mid to late April to mid to late July). These terms are separated by Christmas holidays (two weeks), Easter holidays (two weeks) and summer holidays (six weeks). There is also a mid-term break for each term, which could also be responsible for the dramatic fluctuations of the transmission rates. We observe two comparable dominant frequencies for Manchester: 1/year and 3/year. This implies that both seasonal factors and school terms influence measles transmission in Manchester and the seasonal factors in Manchester do not affect measles transmission as much as that in London. This may be because that Manchester has a relative stable high humidity whereas the humidity in London varies obviously. The relative humidity in London is lower than 80% from March to September and higher than 80% from October to February [1]. In contrast, the relative humidity is above 80% in Manchester all year round and does not show dramatic variation [2]. According to [17], morbidity of measles increases when the relative humidity is low and decreases during the period of high relative humidity. From Figure 4.2 we can also see that there is more noise in the dominant frequencies in Manchester. This may be because the population size in Manchester is much smaller than that in London. Thus, the transmission of measles in London is mainly driven by seasonal weather conditions whereas the transmission of measles in Manchester is affected more by human activities including school terms and some other random factors.

To estimate the probability that the 1/year and 3/ year frequencies observed in Figure 4.2 occurred only by chance, we carry out a significance test based on 1000

repeated experiments. In each experiment, a time series of weekly new infections is created with the reporting rate of each week randomly chosen from $[47\%, 57\%]$ since the mean reporting rate is about 52% [12]. Then the transmission rates are estimated based on the created infection data, and Fourier transform is carried out. The result in Figure 4.3 indicates that for all the 1000 experiments, there are two dominant frequencies for London: 1/year and 3/year, and the 1/year peak is much higher than the 3/year peak, whereas there are two comparable dominant frequencies for Manchester: 1/year and 3/year.

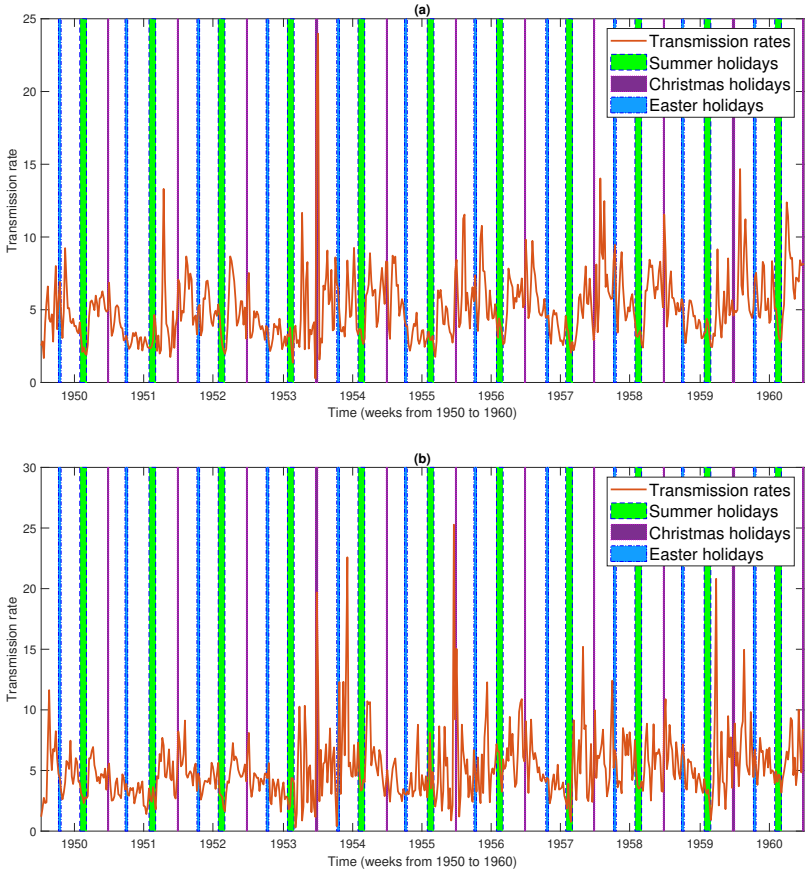

FIG. 4.1. *(a) The estimated transmission rate of measles in* **London** *from 1950 to 1960. (b) The estimated transmission rate of measles in* **Manchester** *from 1950 to 1960.*

5. Application to a disease without obvious periodicity. Some infectious diseases, such as Ebola and COVID-19, do not have obvious periodicity. In this section, we use the discrete inverse method to estimate the transmission rate of SARS-CoV-2 Delta varaint in California under imperfect vaccination. Delta was the predominant SARS-CoV-2 variant strain circulating at a high proportion in the US from August to mid-December 2021 (see supplementary Figure SM0.13). California was one of the most seriously affected states in the US during the pandemic.

Motivated by the models in [36, 35], we propose the following model:

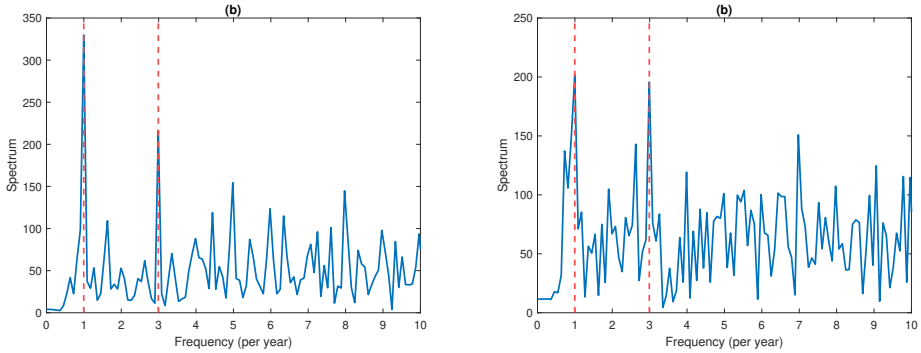

FIG. 4.2. *(a) Modulus of the Fourier transform of the transmission rate in* **London** *from 1950 to 1960. (b) Modulus of the Fourier transform of the transmission rate in* **Manchester** *from 1950 to 1960.*

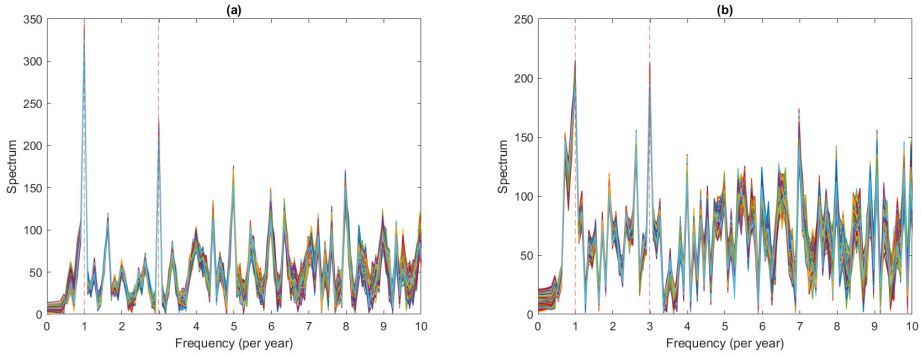

FIG. 4.3. *Significance test of the spectrum peaks at 1/year and 3/year frequencies based on 1000 time series of notified weekly new cases from 1950 to 1960 with reporting rate randomly chosen from* $[47\%, 57\%]$*: (a) Modulus of the Fourier transform of the transmission rate in* **London**. *(b) Modulus of the Fourier transform of the transmission rate in* **Manchester**.

$$
\begin{aligned}
\frac{\mathrm{d}S(t)}{\mathrm{d}t} &= -\beta(t)\frac{S(t)(I(t)+\theta_E E(t)+\theta_A A(t))}{N} - \eta_F(t)S(t),\\
\frac{\mathrm{d}E(t)}{\mathrm{d}t} &= \beta(t)\frac{(S(t)+\epsilon_F V_F(t)+\epsilon_B V_B(t))(I(t)+\theta_E E(t)+\theta_A A(t))}{N} - \delta E(t),\\
\frac{\mathrm{d}I(t)}{\mathrm{d}t} &= (1-p)\delta E(t) - \mu(t)I(t) - r_I I(t),\\
\frac{\mathrm{d}A(t)}{\mathrm{d}t} &= p\delta E(t) - r_A A(t),\\
\frac{\mathrm{d}V_F(t)}{\mathrm{d}t} &= \eta_F(t)S(t) - \eta_B(t)V_F(t) - \frac{\beta(t)V_F(t)\epsilon_F(I(t)+\theta_E E(t)+\theta_A A(t))}{N}\\
\frac{\mathrm{d}V_B(t)}{\mathrm{d}t} &= \eta_B(t)V_F(t) - \frac{\beta(t)V_B(t)\epsilon_B(I(t)+\theta_E E(t)+\theta_A A(t))}{N}\\
\frac{\mathrm{d}R(t)}{\mathrm{d}t} &= r_I I(t) + r_A A(t),\\
\frac{\mathrm{d}D(t)}{\mathrm{d}t} &= \mu(t)I(t).
\end{aligned}
\tag{5.1}
$$

Here the variables $S(t)$, $E(t)$, $I(t)$, $A(t)$, $R(t)$ and $D(t)$ represent the number of susceptible, exposed, symptomatic infectious, asymptomatic infectious, recovered, and dead individuals at time t, respectively. In the US, mass vaccination started on December 20, 2020, and booster vaccines started to be given on August 13, 2021 when Delta variant was the predominant strain. Accordingly, we consider two vaccinated compartments in our model: uninfected fully vaccinated without a booster shot (V_F) and uninfected boosted (V_B). The time-dependent parameter $\beta(t)$ is the transmission rate to be estimated. The parameters θ_E and θ_A are the relative transmissibilities of the exposed and asymptomatic infectious individuals, respectively. The average duration of the incubation period is $1/\delta$. A proportion p of the infected individuals are asymptomatic and hence the symptomatic ones occupy $1-p$. The recovery rates of the symptomatic and asymptomatic infectious individuals are r_I and r_A, respectively. The disease-induced death rate is $\mu(t)$. Since we focus on short-term dynamics (from August to November 2021), we assume that the total population of the US keeps unchanged at N during that period and we do not incorporate a birth rate or a natural death rate in the model. The full vaccination rate and the booster vaccination rate are $\eta_F(t)$ and $\eta_B(t)$, respectively. Since some vaccinated individuals experienced breakthrough infections even with a booster shot, we use ϵ_F and ϵ_B to represent the relative risks of infection for these two vaccinated compartments, respectively.

People infected with the SARS-CoV-2 Delta variant carry higher viral load and become infectious sooner than those infected with the original virus strains, with an average of only four days to reach the virus detectable level [33]. Hence, we assume that $1/\delta = 4$. It is estimated that people infected with Delta variant can be contagious no more than 10 days if they are mildly ill whereas they can be contagious up to 20 days if they are moderately or severely ill [33]. Then we assume that $1/r_I = 15$ and $r_A = 1/7$. We estimate ϵ_F and ϵ_B according to vaccine efficacy. The vaccine effectiveness of the Pfizer–BioNTech BNT162b2 mRNA vaccine against Delta variant is about 88% after the second dose and 94% after the booster dose [11, 32]. Since most people in the US take either Pfizer or Moderna vaccines which have similar efficacy [25], we use the vaccine effectiveness of Pfizer to approximate the values of ϵ_F and ϵ_B which gives $\epsilon_F = 1 - 0.88 = 0.12$ and $\epsilon_B = 1 - 0.94 = 0.06$. Preliminary studies show that both unvaccinated and fully vaccinated, symptomatic and asymptomatic individuals infected with the SARS-CoV-2 Delta variant produce the same amount of virus [5]. So we can assume that the transmissibility of asymptomatic infected individuals is almost the same as that of symptomatic ones, that is, $\theta_A = 1$. Besides, we assume that $\theta_E = 0.1$. Since around a quarter to a third of the individuals who have experienced breakthrough infections are asymptomatic [30], we set $p = 0.25$ by assuming that the asymptomatic proportion is the same among unvaccinated infected population. We take $N = 39237836$ [3].

To estimate the time-varying transmission rate, we start by obtaining the time series of $E(t)$ from the term $(1-p)\delta E(t)$ which can be approximated by the notification data of daily confirmed cases obtained from [29] (see supplementary Figure SM0.15). We use $S[i]$, $E[i]$, $I[i]$, $A[i]$, $V_F[i]$, $V_B[i]$, $R[i]$ and $D[i]$ to represent the values of the variables in model (5.1), and $y[i]$ the notification data of daily confirmed cases, on the i-th day. Then we have

$$E[i] = \frac{y[i]}{(1-p)\delta}, \quad i = 1, 2, 3, ..., K,$$

where K is the length of the time series of notification data. We can obtain the time series of new deaths, breakthrough cases, cumulative fully vaccinated and boosted, and

estimate the initial values $I[1]$, $R[1]$ from the reported data in [4, 29, 38]. Then we can further calculate the time series of $D[i]$, $V_F[i]$, $V_B[i]$, $i = 1, 2, 3, ..., K$. We assume that $A[1] = I[1]/3$. It follows that $S[1] = N - E[1] - I[1] - A[1] - R[1] - D[1] - V_F[1] - V_B[1]$.

Then we can obtain the values of all variables on each day according to the following procedure:

$$\begin{aligned} I[i] &= I[i-1] + (1-p)\delta E[i-1] - (\mu[i-1] + r_I)I[i-1], \\ A[i] &= A[i-1] + p\delta E[i-1] - r_A A[i-1], \\ R[i] &= R[i-1] + r_I I[i-1] + r_A A[i-1], \\ S[i] &= N - E[i] - I[i] - A[i] - R[i] - D[i] - V_F[i] - V_B[i], \end{aligned}$$

for $i = 2, 3, ...K$. Adding up the equations for the S, V_F and V_B compartments, we have

$$\frac{\mathrm{d}(S(t) + V_F(t) + V_B(t))}{\mathrm{d}t} = -\frac{\beta(t)(S(t) + \epsilon_F V_F(t) + \epsilon_B V_B(t))(I(t) + \theta_E E(t) + \theta_A A(t))}{N}.$$

Substituting the time series of $S[i]$, $V_F[i]$, $V_B[i]$, $I[i]$, $E[i]$ and $A[i]$ into the difference form of the above equation, we can solve for $\beta[i]$ as follows:

$$\begin{aligned} \beta[i-1] = &- \frac{N(S[i] + V_F[i] + V_B[i] - S[i-1] - V_F[i-1] - V_B[i-1])}{((S[i-1] + \epsilon_F V_F[i-1] + \epsilon_B V_B[i-1])(\theta_E E[i-1] + \theta_A A[i-1] + I[i-1]))}, \\ i = &2, 3, ..., K, \\ \beta[K] \approx &\beta[K-1]. \end{aligned}$$

The estimated transmission rates in California from August 1, 2021 to November 30, 2021 are shown in Figure 5.1.

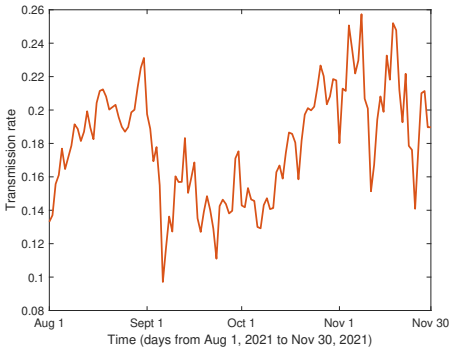

FIG. 5.1. *Transmission rates of COVID-19 in California from August 1, 2021 to November 30, 2021.*

Sensitivity analysis can provide important information as to which factors deserve more attention in controlling the disease. To calculate the sensitivity index of the estimated transmission rates with respect to each constant parameter, we use the normalized forward sensitivity index (see, e.g. [16]):

$$\text{Sensitivity Index (S.I.)} = \frac{\partial \beta(t)}{\partial \text{parameter}} \cdot \frac{\text{parameter}}{\beta(t)}. \tag{5.2}$$

Since there is no explicit formula of $\beta(t)$ in terms of each constant parameter, we use the central difference approximation (see, e.g. [34]) to evaluate the partial derivatives, that is,

$$\frac{\partial\beta(t)}{\partial\text{parameter}} = \frac{\beta(t,\text{parameter}+h)-\beta(t,\text{parameter}-h)}{2h} + O(h^2).$$

Let $h = 1\%$ of the parameter value P. Then equation (5.2) becomes

$$S.I. = \frac{\beta(t,1.01P)-\beta(t,0.99P)}{0.02\beta(t,P)}. \tag{5.3}$$

We also apply the formula (5.3) to analyze the sensitivity of $\beta(t)$ with respect to the initial conditions and input data. To this end, we replace P with the target initial values or time series data in (5.3).

From Figure 5.2 we can see that the sensitivity indices (S.I.) of $\beta(t)$ to some parameters and data vary with time. The S.I. of $\beta(t)$ with respect to p, r_I, r_A, daily confirmed cases data, fully vaccinated data, death data and the initial recovered data are positive. The S.I. of $\beta(t)$ to N, θ_A, and ϵ_F are negative. The S.I. of $\beta(t)$ to the initial symptomatic and asymptomatic infected data are negative in the beginning and $\beta(t)$ becomes less sensitive to them as time passes. The parameters θ_E, ϵ_B, the booster vaccination data and the breakthrough cases data almost have no impact on $\beta(t)$. The S.I. of $\beta(t)$ to δ varies dramatically with time. Note that a positive S.I. does not mean that an increase of the related parameter or data will lead to more serious transmission of the disease in reality. Take the positive S.I. of the transmission rate to the fully vaccinated data as an example. It only indicates that with the same infection and death data and the same parameter values, if more people get vaccinated, then the transmission rate must be larger. This is because more vaccinated people will make fewer people get infected. However, when we calculate the S.I. of $\beta(t)$ to the fully vaccinated data, we fix the infection data as well as other data and parameters at the baseline values instead of the true values corresponding to the changed fully vaccinated data. A similar analysis can be carried out for the sensitivity results of other parameters and data. Compared with other data, the fully vaccinated data have stronger influence on $\beta(t)$. Among all the controllable parameters, r_I, r_A and p have more influence on $\beta(t)$ which implies the importance of treatment and testing since treatment can hopefully improve recovery rate and testing is helpful for identifying the asymptomatic ones.

6. Discussion. In this paper, we developed a new inverse method for deriving the daily or weekly transmission rates based on multi-compartmental ordinary differential equation models and disease incidence data. The method is essentially using forward-Euler discretization of differential equations to generate an iteration process to produce time series of variable values and then derive the time series of transmission rates from one or more equations of the discretized system. The time step is usually one day or one week depending on whether daily or weekly transmission rates need to be estimated. Sometimes such discrete systems may suffer from the issue of instability due to a too large time step. To check the feasibility of the method, we need to verify that the derived transmission rates and compartment variables are all non-negative (see e.g., Figures 3.1, 4.1, 5.1 and supplementary Figures SM0.4, SM0.5, SM0.6, SM0.7, SM0.8, SM0.11,SM0.12,SM0.16). When the term corresponding to notification data of new infections explicitly involves the transmission rate, such as in the flu model (3.1), β can be directly derived from the infection term after we get

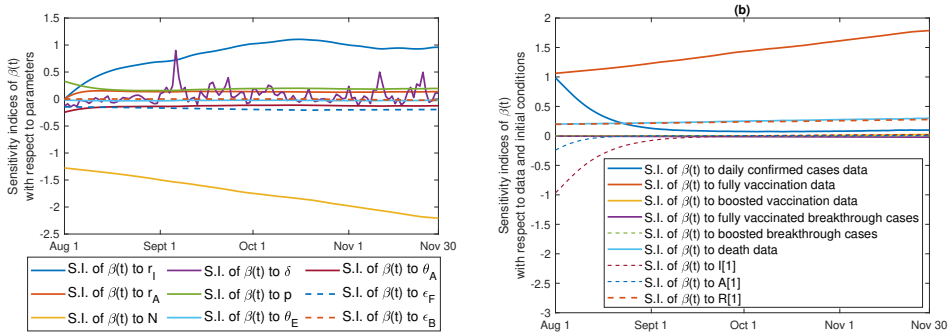

FIG. 5.2. *Sensitivity indices of the transmission rates with respect to (a) the parameters and (b) data and initial conditions in California from August 1, 2021 to November 30, 2021.*

time series of the variables. When the term representing notified new infections does not involve the transmission rate explicitly, such as in the measles model (4.1) and the COVID-19 model (5.1), normally the equation corresponding to the rate of change of the susceptible population is needed to derive the transmission rates once the time series of all variable values are obtained. Thus, the key step is to construct the time series of the susceptible population from those of the other compartments. When it involves long-term dynamics (multiple years or decades) under dramatic population variations, we can either compute the transmission rates year by year using different initial values for different years (see Section 3) or estimate the transmission rates for the entire period of interest with one initial value for each variable (see Section 4). A birth rate and a natural death rate need to be incorporated for the latter case.

We introduced the discrete inverse method based on a general SIS model and found that the inverse method based on forward Euler discretization is the best in both accuracy and speed of computation. We applied the method to extract transmission rates from notification data of confirmed cases for three diseases: flu, measles and COVID-19 which are selected for study according to their different cycles. For each application, we discussed insights gained about specific epidemiological issues. Based on Fourier transform of the transmission rates for flu in the US, we verified it as a seasonal disease. We also found that the transmission rates of flu within each year vary dramatically in more recent years. Moreover, the risk of infection with flu is highest in Decembers from 2013 to 2018 and protection measures against flu are worth taking as early as in August each year in the US. A better exploration for flu transmission should be conducted as a regional study within a state, which allows for connecting the transmission rates with weather conditions. That requires the collection and publication of state-wide or county-wide ILI data and vaccination data. By comparing the Fourier transforms of the transmission rates of measles in London and Manchester, we found that both seasonal conditions, such as humidity, and school terms contribute significantly to the transmission of measles. In Manchester, the modulator "school dates" is more important than that in London. In addition, the dominant frequencies in London have less noise than those in Manchester because London has a larger population than Manchester, which implies that the results for London are less sensitive to unexpected factors. The method can also be applied to post-vaccination data of measles as a future work. For COVID-19, we estimated the transmission rates of the Delta variant strain in California of the USA. The sensitiv-

ity analysis results show that the fully vaccinated data, the recovery rates and the proportion of asymptomatic infections can all greatly impact the transmission rates, which implies the importance of vaccination, treatment and testing in the control of COVID-19. Model (5.1) can be modified to include multiple SARS-CoV-2 variant strains and applied to smaller regions to mitigate the effect of heterogeneity. In that case, regional data and more parameter values need to be known in order to improve the accuracy of the estimated transmission rates. Another interesting future work is to explore what the obtained $\beta(t)$ imply if we consider the proportion transition of variants in supplementary Figure SM0.13.

Note that in addition to the notification data of new infections, sometimes we also need to incorporate time series data of some other variables in order to make the method work. The principle is that as long as relevant data corresponding to some term (e.g., cumulative deaths) in a model is available it is always better to use the data directly. However, if no data is available, then we need to estimate the related parameters (e.g., from published references or medical information) and run the iteration algorithm to derive time series of the variable. For the SIS model, we only used data of new infections per unit time. For the flu model, we used weekly data of new infections, new vaccinated, and new deaths. For the measles model, we used weekly data of new infections. For the COVID-19 model, we used data of daily new infections, cumulative vaccinated and breakthrough cases, and cumulative deaths.

Our method is totally data-driven and hypothesis-free in the sense that we do not need to make assumptions on the form of the transmission rates. This is different from some traditional methods such as the least squares method which typically assumes the transmission rates to be constant during a specific time period or to take some pre-determined function forms without any validation. In addition to available time series of epidemiological data (e.g., incidence, vaccinated, etc.), the only prerequisites of our method are the initial values of the variables which can be estimated from public health databases, whereas the algorithm of the continuous inverse method in [27] requires an estimation of $\beta(0)$ which is quite challenging or even impossible in reality. Another advantage of our discrete inverse method over the continuous version in [27] is that we do not need to first interpolate the data with a trigonometric function or a spline and we do not need to solve a Bernoulli equation whose coefficients may involve higher order derivatives of the smooth function of prevalence data (see, e.g., supplementary Theorem SM0.1). Our iteration algorithm only uses discrete data instances without any complicated integrals in the formula for $\beta(t)$, which greatly simplifies the computation process and makes our method much faster in obtaining the estimated transmission rates. This advantage is particularly obvious when the disease has an incubation period and the incidence term in the equation for the exposed compartment is not used as the term corresponding to notification data. For example, we assumed that the notified measles incidence frequency data coincide with the time series of $aE(t)$ instead of $\beta(t)S(t)I(t)$ in model (4.1) and we use the term $(1-p)\delta E(t)$ instead of $\beta(t)(S(t)+\epsilon_F V_F(t)+\epsilon_B V_B(t))(I(t)+\theta_E E(t)+\theta_A A(t))/N$ as the notification term in model (5.1). In these cases, the continuous inverse method in [27] will produce a rather complicated expression for $\beta(t)$, which dramatically reduces the speed of computation. From supplementary Remarks SM0.3 and SM0.4, we can imagine how laborious it is to apply the continuous inverse method to the measles model (4.1) and the COVID-19 model (5.1). In contrast, our method runs fast for all the three models even when $aE(t)$ and $(1-p)\delta E(t)$ are used as the notification terms of new infections in models (4.1) and (5.1), respectively. As a byproduct, we suggested a faster method to derive the transmission rates with the continuous inverse method by directly using

ode45 in MATLAB when the notified new infection terms explicitly depends on $\beta(t)$ (see Remark 2.2). However, it is still a little slower than our discrete inverse method based on a comparison for the SIS model and the flu model (see Tables 2.1 and 3.2).

One promising application of the discrete inverse method is to provide the estimated transmission rate as the response variable for some machine learning models to forecast disease incidence under the impact of some predictor variables such as human mobility trends and non-pharmaceutical interventions which affect the transmission rate either directly or indirectly. This can be realized by developing a hybrid model consisting of a mechanistic model and a machine learning model (see, e.g., [36, 35]). When combined with machine learning, an accurate estimation of transmission rates allows for effective training which may produce reliable testing/predictions and enables the most influential predictor variables to be identified. Derivation of transmission rates using the discrete inverse method can also help analyze control outcomes in the past to gain experience or learn lessons for taking mitigation measures in the future. Different interventions usually lead to different trends in human mobility and, as a result, different transmission rates. Thus, policymakers could select one set of intervention policies that will control the disease to the best by comparing different transmission scenarios under different combinations of future interventions.

Mechanistic models can do far more than just forecasting disease incidence and the discrete inverse method can be applied to a variety of infectious diseases as well. In practice, data availability and quality are important for the implementation of our method. Data scarcity is a typical problem for newly emerging infectious diseases, especially at the initial stage of an epidemic or pandemic. Moreover, the notification data may underestimate the actual number of infections if infected people are not diagnosed due to unawareness (e.g., asymptomatic infections) or underdeveloped tracking and testing systems. On the one hand, effective data collection and surveillance technologies need to be harnessed, particularly in disadvantaged regions where more funding should be targeted. On the other hand, future models must account for underreporting and missing data in order to facilitate disease transmission mechanisms research and inform control strategies. When data on other compartments (such as quarantined and hospitalized) are available, the models may be able to provide a more accurate estimate of the transmission rates by incorporating extra compartments. Besides, the discrete inverse method also works when prevalence data are available. In that case, we can directly employ a time series of currently infected population to derive the time series of the other variables. In addition to ordinary differential equation models, our method can be applied to difference equations as well since our method is basically based on discretized differential equations. It is also intriguing to apply the method to some disease models represented by delay differential equations, partial differential equations or stochastic differential equations. Furthermore, the approach in this paper can be generalized to deduce some time-varying parameters of other epidemiological, immunological, ecological and social compartmental models based on laboratory or field data, and may be informative in approximating a specific function form of the estimated parameter (e.g., the Holling-type functional responses), which may be of interest to a broad community that includes not only applied mathematicians but also biologists, biomedical engineers, clinicians and others with a quantitative mindset.

Acknowledgments. The authors would like to thank the three anonymous reviewers for their insightful suggestions and comments which led to a substantial improvement of the manuscript.

675 REFERENCES

676 [1] *Average humidity in London (Greater London)*, 2022, https://weather-and-climate.com/
677 average-monthly-Humidity-perc,London,United-Kingdom (accessed 2022-05-18).
678 [2] *Average humidity in Manchester (Greater Manchester)*, 2022, https://weather-and-climate.
679 com/average-monthly-Humidity-perc,Manchester,United-Kingdom (accessed 2022-05-18).
680 [3] *California population*, 2022, https://www.populationu.com/us/california-population (accessed
681 2022-05-18).
682 [4] *Covid-19 post-vaccination infection data*, 2022, https://data.chhs.ca.gov/dataset/
683 covid-19-post-vaccination-infection-data (accessed 2022-11-12).
684 [5] C. B. Acharya, J. Schrom, A. M. Mitchell, et al., *No significant difference in viral load*
685 *between vaccinated and unvaccinated, asymptomatic and symptomatic groups infected with*
686 *SARS-CoV-2 Delta variant*, medRxiv preprint, (2021), https://doi.org/10.1101/2021.09.
687 28.21264262.
688 [6] L. J. S. Allen, *Some discrete-time SI, SIR and SIS epidemic models*, Math. Biosci., 124
689 (1994), pp. 83–105, https://doi.org/10.1016/0025-5564(94)90025-6.
690 [7] R. M. Anderson and R. May, *Infectious Diseases of Humans*, Oxford University Press–
691 Oxford, 1991.
692 [8] R. E. Baker, A. S. Mahmud, I. F. Miller, et al., *Infectious disease in an era of global*
693 *change*, Nature Reviews Microbiology, 20 (2022), pp. 193–205, https://doi.org/10.1038/
694 s41579-021-00639-z.
695 [9] A. D. Becker, A. Wesolowski, O. N. Bjørnstad, and B. T. Grenfell, *Long-term dynamics*
696 *of measles in London: Titrating the impact of wars, the 1918 pandemic, and vaccination*,
697 PLoS Comput Biol, 15 (2019), p. e1007305, https://doi.org/10.1371/journal.pcbi.1007305.
698 [10] J. Bedford, J. Farrar, and C. Ihekweazu, *A new twenty-first century science for ef-*
699 *fective epidemic response*, Nature, 575 (2019), pp. 130–136, https://doi.org/10.1038/
700 s41586-019-1717-y.
701 [11] J. L. Bernal, N. Andrews, C. Gower, et al., *Effectiveness of Covid-19 vaccines against the*
702 *B.1.617.2 (Delta) variant*, The New England Journal of Medicine, 385 (2021), pp. 585–594,
703 https://doi.org/10.1056/NEJMoa2108891.
704 [12] O. N. Bjørnstad, B. F. Finkenstädt, and B. T. Grenfell, *Dynamics of measles epidemics:*
705 *Estimating scaling of transmission rates using a time series SIR model*, Ecol. Monogr., 72
706 (2002), pp. 169–184, https://doi.org/10.2307/3100023.
707 [13] B. Bolker, *Measles data*, 2014, https://ms.mcmaster.ca/~bolker/measdata/ewcitmeas.dat
708 (accessed 2022-03-14).
709 [14] Centers for Disease Control and Prevention, *Measles*, 2020, https://www.cdc.gov/
710 measles/hcp/index.html (accessed 2022-03-14).
711 [15] Centers for Disease Control and Prevention, *Influenza (flu)*, 2022, https://www.cdc.
712 gov/flu/index.htm (accessed 2022-03-14).
713 [16] N. Chitnis, J. M. Hyman, and J. M. Cushing, *Determining important parameters in the*
714 *spread of malaria through the sensitivity analysis of a mathematical model*, Bull. Math.
715 Biol., 70 (2008), pp. 1272–1296, https://doi.org/10.1007/s11538-008-9299-0.
716 [17] J. G. de Jong and K. C. Winkler, *Survival of measles virus in air*, Nature, 201 (1964),
717 pp. 1054–1055, https://doi.org/10.1038/2011054a0.
718 [18] K. P. Hadeler, *Parameter identification in epidemic models*, Math. Biosci., 229 (2011),
719 pp. 185–189, https://doi.org/10.1016/j.mbs.2010.12.004.
720 [19] J. D. Kong, C. Jin, and H. Wang, *The inverse method for a childhood infectious disease model*
721 *with its application to pre-vaccination and post-vaccination measles data*, Bull. Math. Biol.,
722 77 (2015), pp. 2231–2263, https://doi.org/10.1007/s11538-015-0121-5.
723 [20] MacroTrends, *London, UK metro area population 1950-2022*, 2022, https://www.
724 macrotrends.net/cities/22860/london/population (accessed 2022-05-17).
725 [21] MacroTrends, *Manchester, UK metro area population 1950-2022*, 2022, https://www.
726 macrotrends.net/cities/22862/manchester/population (accessed 2022-03-02).
727 [22] MacroTrends, *U.K. life expectancy 1950-2022*, 2022, https://www.macrotrends.net/
728 countries/GBR/united-kingdom/life-expectancy (accessed 2022-03-14).
729 [23] M. E. Martinez, *The calendar of epidemics: Seasonal cycles of infectious diseaess*, PLoS
730 Pathog, 14 (2018), p. e1007327, https://doi.org/10.1371/journal.ppat.1007327.
731 [24] A. Mubayi, A. Pandey, C. Brasic, A. Mubayi, P. Ghosh, and A. Ghosh, *Analytical estima-*
732 *tion of data-motivated time-dependent disease transmission rate: An application to Ebola*
733 *and selected public health problems*, Tropical Medicine and Infectious Disease, 6 (2021),
734 p. 141, https://doi.org/10.3390/tropicalmed6030141.
735 [25] P. Olliaro, E. Torreele, and M. Vaillant, *Covid-19 vaccine efficacy and effectiveness -*

the elephant (not) in the room, Lancet Microbe, 2 (2021), pp. e279–e280, https://doi.org/10.1016/S2666-5247(21)00069-0.

[26] OPCS, *The registrar general's quarterly or annual reports and various English census reports 1948-1967*, The weekly OPCS (Office of Population Censuses and Surveys) reports, (1967).

[27] M. Pollicott, H. Wang, and H. H. Weiss, *Extracting the time-dependent transmission rate from infection data via solution of an inverse ODE problem*, J. Biol. Dyn., 6 (2012), pp. 509–523, https://doi.org/10.1080/17513758.2011.645510.

[28] PopulationPyramid.net, *Population pyramids of the world from 1950 to 2100*, 2019, https://www.populationpyramid.net/united-kingdom/1950/ (accessed 2022-05-18).

[29] H. Ritchie, E. Mathieu, L. Rodés-Guirao, et al., *Coronavirus pandemic (COVID-19). Our World in Data*, 2020, https://ourworldindata.org/coronavirus (accessed 2022-03-03).

[30] Sara Berg, *What doctors wish patients knew about breakthrough COVID infections*, 2022, https://www.ama-assn.org/delivering-care/public-health/what-doctors-wish-patients-knew-about-breakthrough-covid-infections (accessed 2022-03-03).

[31] J. Shaman and A. Karspeck, *Forecasting seasonal outbreaks of influenza*, PNAS, 109 (2012), pp. 20425–20430, https://doi.org/10.1073/pnas.1208772109.

[32] M. G. Thompson, K. Natarajan, S. A. Irving, et al., *Effectiveness of a third dose of mRNA vaccines against COVID-19-associated emergency department and urgent care encounters and hospitalizations among adults during periods of Delta and Omicron variant predominance - vision network, 10 states, August 2021 - January 2022*, MMWR Morb Mortal Wkly Rep, 71 (2022), pp. 139–145, https://doi.org/10.15585/mmwr.mm7104e3externalicon.

[33] UCHealth, *The Delta variant*, https://www.uchealth.org/services/infectious-diseases/coronavirus-covid-19/the-delta-variant-of-covid-19/ (accessed 2022-03-02).

[34] X. Wang, H. Wang, and M. Y. Li, *R_0 and sensitivity analysis of a predator-prey model with seasonality and maturation delay*, Math. Biosci., 315 (2019), p. 108225, https://doi.org/10.1016/j.mbs.2019.108225.

[35] X. Wang, H. Wang, P. Ramazi, K. Nah, and M. A. Lewis, *From policy to prediction: Forecasting COVID-19 dynamics under imperfect vaccination*, Bull. Math. Biol., (2022), https://doi.org/10.1007/s11538-022-01047-x.

[36] X. Wang, H. Wang, P. Ramazi, K. Nah, and M. A. Lewis, *A hypothesis-free bridging of disease dynamics and non-pharmaceutical policies*, Bull. Math. Biol., 84 (2022), https://doi.org/10.1007/s11538-022-01012-8.

[37] World Health Organization, *Measles*, 2019, https://www.who.int/news-room/fact-sheets/detail/measles (accessed 2022-03-14).

[38] Worldometer.info, *United States coronavirus cases, deaths, recovered*, 2019, https://www.worldometers.info/coronavirus/country/us/ (accessed 2022-03-03).